In Situ Measurements of Organics, Meteoritic Material, Mercury, and Other Elements in Aerosols at 5 to 19 Kilometers

D. M. Murphy*, D. S. Thomson, M. J. Mahoney

In situ measurements of the chemical composition of individual aerosol particles at altitudes between 5 and 19 kilometers reveal that upper tropospheric aerosols often contained more organic material than sulfate. Although stratospheric aerosols primarily consisted of sulfuric acid and water, many also contained meteoritic material. Just above the tropopause, small amounts of mercury were found in over half of the aerosol particles that were analyzed. Overall, there was tremendous variety in aerosol composition. One measure of this diversity is that at least 45 elements were detected in aerosol particles. These results have wide implications for the complexity of aerosol sources and chemistry. They also offer possibilities for understanding the transport of atmospheric aerosols.

Understanding the composition of atmospheric aerosol particles is necessary for identifying their sources and predicting their effects on atmospheric chemistry and climate. Aerosols influence Earth's heat budget both directly by absorbing and scattering sunlight, and indirectly by acting as nuclei for cloud droplets. These aerosol effects are responsible for some of the most important uncertainties associated with global-mean radiative forcing (*1*). Aerosols also affect gas phase chemistry through heterogeneous processes. In the stratosphere, aerosols take up nitric acid and water at cold temperatures to form polar stratospheric clouds, which play a major role in polar ozone depletion (*2*). Heterogeneous reactions are known to affect the NO_x budget throughout the lower stratosphere and have been suggested as a way of resolving discrepancies in the NO_x budget of the upper troposphere. Recent changes in various anthropogenic and natural species in the atmosphere could affect the number, size, and composition of aerosols and in turn influence atmospheric chemical cycles. Increased air traffic is of special concern for injecting material that could affect aerosols at high altitudes (*3*).

It has been known since the 1960's that the stratospheric aerosol layer consists mostly of sulfate and associated water (*4*). An early suggestion that many stratospheric aerosols contain meteoritic material (*5*) was later disputed (*6*). A few percent of stratospheric particles have been shown to have diverse compositions including soot and minerals (*7*). Aerosols in the upper troposphere are not as well characterized as those in the lower stratosphere. Most modeling studies have assumed that upper tropospheric aerosols are either ammonium sulfate or sulfuric acid.

Measurements of volatile or trace species in stratospheric aerosols have been scarce. Temperatures at 12 to 19 km altitude are usually less than 225 K. Bringing either filter samples or electron microscope grids back for laboratory analysis at room temperature thus involves heating the samples by more than 75 K. Such heating risks significant changes in composition. Sulfuric acid aerosols also readily take up ammonia and organics from the air (*8, 9*). Therefore, sample handling can easily affect those species. Here we report in situ measurements of the composition of stratospheric aerosols, which minimize volatization and contamination of aerosols, and discuss their implications for atmospheric chemistry and dynamics.

Method

Aerosol particles were analyzed using a laser ionization mass spectrometer (PALMS) mounted in the nose of a WB-57F high altitude research airplane (*10*). Aerosols are brought into a vacuum system and individual particles are detected by light scattered as they cross the beam of a continuous laser. The scattered light signal gives a rough indication of the size of the particle and a trigger for an excimer laser (193 nm), which is pulsed so its beam hits the particle to desorb and ionize molecules and atoms. These ions are analyzed with a time of flight mass spectrometer to provide a complete mass spectrum from each particle. By changing the acceleration voltages, the mass spectrometer can transmit either positive or negative ions to the detector. The polarity was changed every few minutes in flight; about two-thirds of the time was spent acquiring positive spectra. Laser pulses with no aerosols present produced less than 0.1% of the signal from a typical particle, and thus the spectra are representative of aerosol species only. For example, the system is sensitive to aerosol nitrate but not to gas phase nitric acid.

Calibrations with KCl particles and latex spheres indicate that the flight instrument could not detect particles with diameters less than about 0.2 μm. Particles larger than 2 μm included most of the aerosol mass during these flights but usually only a minority of the number of particles (*11*). Except during time spent in cirrus clouds, mass spectra were obtained from over 90% of valid triggers. Therefore, we can be confident that these data include all of the common types of aerosols larger than 0.2 μm.

These mass spectra, with signal-to-noise ratios that often exceed 1000, are more sensitive to many trace species than previous techniques used to analyze stratospheric aerosols. Artifacts are minimized because the particles never touch a surface and because the main inlet into the aircraft, which is nearly isokinetic, is within an estimated 5 K of ambient temperatures. Analysis was complete less than 7 ms after the aerosols entered the aircraft and less than 1 ms after the aerosols entered the vacuum chamber. Although that is more than enough time for evaporation or condensation of monolayers of volatile species, mass transfer calculations indicate that there should not be any changes in the bulk composition of aerosols. Spectra of water were observed in cirrus clouds, indicating that at least some of even the most volatile particles survived into the instrument.

Flights were made from Houston during April and May 1998, a time of minimal volcanic influence on stratospheric aerosols.

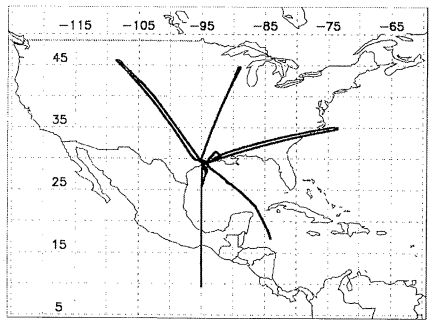

Fig. 1. Flight tracks of the WB-57F Aerosol Mission. Two flights were flown down the 95°W meridian.

D. M. Murphy and D. S. Thomson, Aeronomy Laboratory, National Oceanic and Atmospheric Administration, 325 Broadway, Boulder, CO 80303, USA. M. J. Mahoney, Jet Propulsion Laboratory MS 246–101, California Institute of Technology, 4800 Oak Grove Drive, Pasadena, CA 91109, USA. E-mail: murphyd@al.noaa.gov

*To whom correspondence should be addressed.

Flights covered latitudes from 9°N to 46°N and altitudes up to 19 km (Fig. 1). Mass spectra were obtained from over 28,000 individual particles. A microwave temperature profiler (MTP) on the WB-57F measured the temperature above and below the airplane (*12*). The position of the tropopause was then derived from the temperature profiles using the WMO definition for the thermal tropopause.

Sulfate and Organics

Most of the negative ion spectra of stratospheric aerosols were simple (Fig. 2A). Sulfate was the predominant component. Only a few percent of the aerosols had compositions in which sulfate was not dominant, in agreement with data from Sheridan *et al.* (*7*). In the upper troposphere, many of the negative ion spectra were more complicated (Fig. 2B). Organic peaks were common. Organics and sulfates were usually present in the same particles (internally mixed). Besides the particle and aerosol types shown in Fig. 2, negative ion spectra of mineral and soot particles were also observed. These were occasionally present well above the tropopause but were more common in the troposphere.

It is difficult to convert the peak areas observed in laser ionization spectra to mass fractions because the efficiency with which different species form ions can vary by large factors. For example, only 0.1% of the organics in sulfuric acid generated over 50% of the positive ions (*9*), but the sensitivities for similar ions such as Cl^- and Br^- in sea salt can be within factor of 2 of each other (*13*). Calibrations with known aerosols are the best way to quantify the spectra, and a few are available. Furthermore, in the absence of matrix effects, the changes in percentages of given ions in different spectra can indicate trends in the abundances of some species even without knowing the absolute mass fractions.

Average profiles of the sulfate and organic peaks, expressed as percentages of the total ion current, show that the tropopause was associated with a distinct change in aerosol composition (Fig. 3). In the stratosphere, sulfate peaks dominated the negative ion spectra. As in Fig. 2A, the remaining negative ions were mostly O^- and OH^-. Positive ion spectra, which are much more sensitive to organics, demonstrate the presence of a small but non-zero concentration of organics in stratospheric aerosols. In the upper troposphere, organic ions were often more abundant than sulfate ions in negative ion spectra. Laboratory calibrations show that the negative ion spectra are more sensitive to sulfate than to organics. Therefore, the sulfate ion data in Fig. 3 are most likely upper limits for the mole percentages of sulfate.

Meteoritic Material in Stratospheric Aerosols

Iron was present in about half of the spectra of stratospheric aerosols, and was often the largest positive ion peak (Fig. 4A). The ^{54}Fe and ^{56}Fe isotopes allow us to identify iron with confidence. Peaks such as $H_3SO_4^+$ in the spectra indicate that the iron was present in sulfate aerosols. Because metals make positive ions much more readily than sulfate does, even small mole fractions of metals can be easily observed in the positive ion spectra of stratospheric sulfate aerosols.

Two types of evidence indicate that most of the iron in stratospheric aerosols represents meteoritic material. First, spectra with large iron peaks were much more common in the stratosphere than in the troposphere (Fig. 5). Although calibrations are required to convert ion fractions to mass fractions, the shift in Fig. 5 is sufficiently large to conclude that the fractional iron content of aerosols is larger in the stratosphere than in the troposphere. This difference indicates a high altitude source of iron. Second, the iron-containing stratospheric aerosol particles also contained magnesium and other elements (Na, Al, K, Ca, Cr, and Ni) in proportions that are consistent with meteoritic material (*14*). For example, the $^{39}K/^{23}Na$ ion ratio in stratospheric particles containing iron is quite distinct from the larger and much more variable ratio at lower altitudes (Fig. 6). The $^{39}K/^{23}Na$ ion ratio from stratospheric aerosols is close to the ion

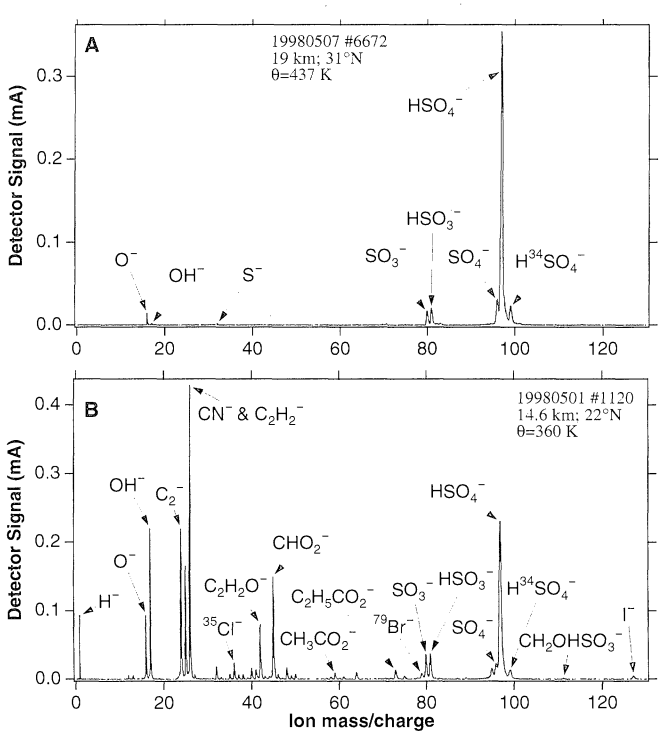

Fig. 2. Examples of negative ion spectra obtained from single aerosol particles in (**A**) the stratosphere and (**B**) the upper troposphere. These spectra were typical of the most common spectra observed in each altitude range. The stratospheric particle spectrum also had a peak at 195 = $H_2SO_4 \cdot HSO_4^-$. The tropospheric particle spectrum shows organic and sulfate peaks along with halogens. The presence of organic acids and $CH_2(OH)SO_3^-$, which is most likely a fragment of hydroxymethanesulfonic acid (HMSA) (*38*), may indicate a role of liquid cloud processing of this particular aerosol.

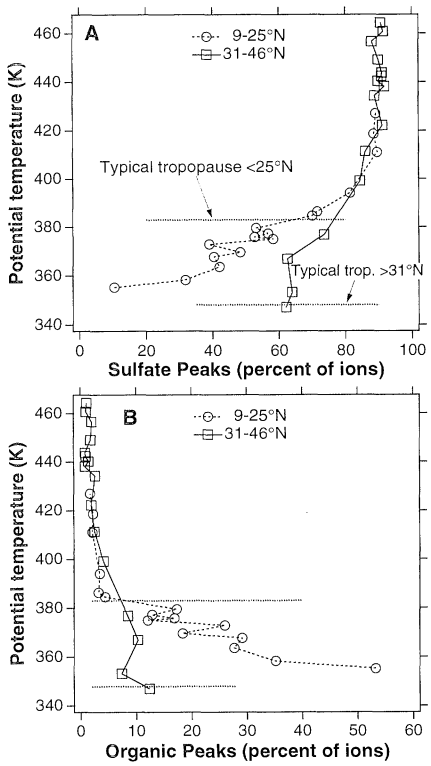

Fig. 3. Average profiles of the percentage of ion current in sulfate (**A**) and organic (**B**) peaks as a function of potential temperature. Each spectrum was normalized to a total ion current of 100%, the spectra were sorted according to the independent variable (here potential temperature) and then the sums of characteristic peaks were averaged over about 270 spectra. Several sulfur-containing peaks were summed for the sulfate signal, of which the most abundant was 97 (HSO_4^-). Mass to charge ratios of 12, 13, 24, 25, 26, 27, 42, 43, 45, and 89 were used as a set of common organic peaks, of which the most abundant was 26 (CN^- and $C_2H_2^-$).

ratio measured at about 100 km altitude after the 1976 Perseid meteor shower (*15*). The larger and more variable tropospheric ratios are consistent with sources such as mineral dust. The average iron signal from stratospheric aerosols was not correlated with the particle size estimated from the scattered light pulse.

Most of the mass influx of meteors to Earth is in particles less than 1 mm in diameter that ablate at altitudes above 75 km (*16, 17*). These thus provide a source for metal atoms in the upper atmosphere that eventually recombine to form "smoke" particles estimated to be less than 20 nm in diameter (*16*). Although the free atoms, especially Na, can be detected (*18*), the condensed particles are not easily observed. Presumably, the smoke particles undergo coagulation as the mesospheric air descends followed by the uptake of sulfuric acid and water in the stratosphere. By the time the material has descended to 40 km, free metal atoms are no longer observable (*19*). Meteoritic smoke particles are expected to be very homogeneous in composition (*16*), and coagulation should further homogenize them. Our spectra of stratospheric aerosols are consistent with a very homogeneous material. For example, $^{24}Mg/^{56}Fe$ ratios in the spectra of stratospheric aerosols had a standard deviation of 50% of the mean ratio. This is as constant as the peak ratios we obtained from laboratory salt aerosols that were nominally identical from one particle to the next.

Mercury

Surprisingly, many high altitude particles contained mercury. As shown in Fig. 4C, mercury can be identified unambiguously from its isotopic pattern. Aerosols containing mercury were most common just above the tropopause (Fig. 7). Mercury was present in small amounts in about half of these particles. Over 70% of the spectra collected during one flight leg near the tropopause south from Houston to 10°N contained mercury. Because the mercury peaks were often near the detection limit, an even larger fraction of particles may have contained mercury. In contrast to these results, no mercury was detected in over 1600 positive-ion spectra taken with PALMS at a remote continental surface site and a remote marine surface site (Idaho Hill, Colorado, and Cape Grim, Tasmania). The Hg^+ signal was positively correlated with the particle size estimated from the scattered light, although correlations involving peaks so near the detection limit must be treated with caution.

Mercury and some important mercury compounds are semivolatile (*20*). Because of its long atmospheric lifetime, condensation onto aerosols is thought to be an important sink for atmospheric mercury even though only about 1% of atmospheric mercury at low altitudes is in aerosols (*21*). The strong gradient in aerosol mercury at the tropopause could be a result of the conversion of mercury to less volatile forms in the stratosphere. It cannot be attributed to simple condensation, as the vapor pressure of mercury at 190 K is about 3×10^{-9} mbar (*22*), approximately 100 times the partial pressure expected if there were 2 parts per trillion (ppt) by mass of atomic mercury in the gas phase (*21, 24*) at the tropopause. Atomic mercury reacts slowly with O_3 to form HgO (*24*), which has a low enough vapor pressure to condense at concentrations of parts per trillions (*20*). More work is required to establish whether the reaction with O_3 can account quantitatively for the gradient of particulate Hg above the tropopause. Other possible explanations for the gradient above the tropopause are that the change in overall aerosol composition could change the ionization efficiency of condensed mercury or that condensed mercury could be present at the tropopause but on aerosol particles too small for PALMS to detect. Small aerosol particles (<200 nm across, that is below our detection limit) are especially abundant near the tropical tropopause (*25*) and coagulate in the lower stratosphere.

The expected concentration of mercury in aerosols above the tropopause can be estimat-

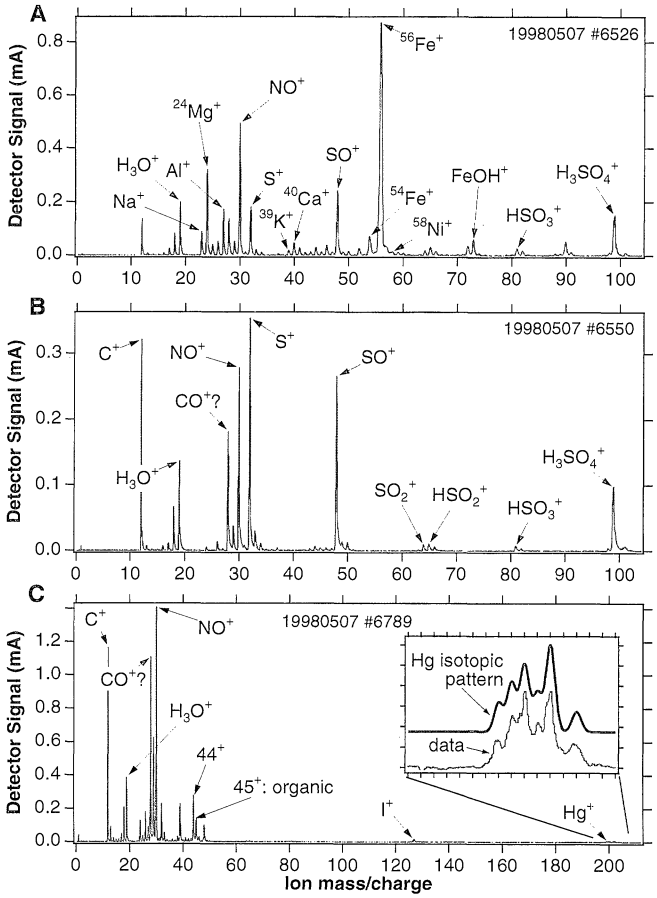

Fig. 4. Several common types of positive ion spectra in the stratosphere. The most common type contained iron, magnesium, and other metals as well as sulfate (**A**). About half of the stratospheric spectra had a large Fe peak. Between 20 and 40% of the spectra obtained more than 2 km above the tropopause showed little Fe, Hg, K, or other metals (**B**). Some organic material and NO^+ was almost always present. Some particles contained mercury (**C**), usually with a distinctive pattern of other peaks including a large C^+ peak and a peak at $m/z = 127$ that is presumed to be I^+. The inset in (C) shows an expanded plot of the data along with the natural isotopes of Hg convoluted with the resolution of the mass spectrometer. These spectra were obtained within minutes of each other in an otherwise fairly homogeneous air mass at 19 km, 31.5°N, and a potential temperature of about 440 K.

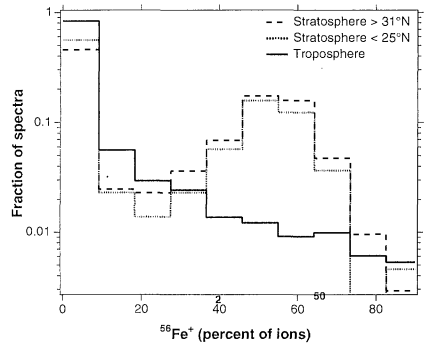

Fig. 5. Frequency of iron in positive ion spectra. The leftmost bin includes spectra with no iron signal. A mass to charge ratio of 56 was nearly unique for iron, as could be verified with measurements of $^{54}Fe^+$. Stratospheric data were defined as those at potential temperatures greater than 410 K and tropospheric data as potential temperatures less than 380 K and at least 600 m below the tropopause measured by the MTP. Aerosols that contain iron were more frequent in the stratosphere than in the upper troposphere. There were insufficient data in the troposphere to separate the histograms by latitude.

ed as 0.1% by mass in that there is approximately 2 ppt by mass of condensible mercury and approximately 2 ppb by mass of aerosol measured just above the tropopause (*11*). Laser ionization mass spectrometers are relatively insensitive to mercury (*26*), in part because of its high ionization potential (10.4 eV). The Hg ion signal shown in Fig. 7 is thus larger than expected. Calibrations for laser ionization of mercury at 193 nm are needed to better constrain the concentration of mercury in aerosols.

Aerosol Diversity

Besides some of the more common types of particles presented in Figs. 2 and 4, there were probably over a hundred less common types of particles, two of which are shown in Fig. 8. The presence of meteoritic material, mercury, organics, and a wide variety of unusual particles means that many elements are present in aerosol particles (Fig. 9). The most common mass peaks were sulfates, organics, and NO^+, and thus H, C, O, N, and S were found in almost every particle. The elements Na, Mg, Al, K, Ca, Cr, Fe, and Ni were commonly measured with the meteoritic material. Halogens were found in many particles in the upper troposphere (Fig. 2B), and also in some stratospheric aerosols. At least 45 elements were found in aerosol particles above 5 km. Of these, about 35 elements were found in the stratosphere.

A few of the rarer elements merit special comments. Boron was observed in about 4% of the spectra and was observed at all altitudes and latitudes. Its sources and aerosol chemistry are not well known. Barium was present in a high fraction of particles during a few short stretches of flight just below the tropopause, mostly south of Houston. Particles containing rubidium almost always had a much larger potassium peak. Lead was significantly more common than the other heavy metals besides mercury. Bismuth was present in a few particles in the stratosphere, where it is thought to come from volcanic material (*27*).

Discussion

The observation that organics can contribute more mass than sulfate to aerosols in portions of the upper troposphere is significant both for the mass balance of aerosols in the troposphere and for the optical and cloud nucleation properties of aerosols. There are few data on organic aerosols in the free troposphere. Our data are consistent with those of Novakov *et al.* (*28*), who found that organics contributed a majority of the aerosol mass at 2 to 3 km over the North Atlantic. Organics are likely to be important for the optical properties of upper tropospheric aerosols. Satellite retrievals that treat aerosols only as sulfuric acid or ammonium sulfate may not give adequate results.

The concentration of meteoritic material in stratospheric aerosols is too low to change the refractive index significantly, but meteoritic material may be important for optical properties if it absorbs light at certain wavelengths. Also, meteoritic material could possibly affect the nucleation of stratospheric aerosols. Recent work has shown that a large fraction of air descending from the mesosphere into the stratosphere is concentrated in the winter polar regions (*29*), where large numbers of aerosols less than 0.1 μm in diameter have been observed (*30*). Our data suggest that many of these particles may contain meteoritic material. Although Zhao *et al.* (*31*) concluded that there would be large numbers of aerosols in the polar stratosphere with or without meteoritic input, a coagulation model applied to aircraft exhaust found that stratospheric size distributions can be sensitive to the initial nuclei (*32*). One must ask if the size distribution of sulfuric acid aerosols and hence the surface area available for heterogeneous processes in the stratosphere is sensitive to the presence of meteoritic nuclei.

Measurements of stratospheric aerosols may provide useful constraints on estimates of the influx of meteoritic material into the earth's atmosphere, which range from 2 to over 40 Gg yr^{-1} (*17, 33*). For comparison, a source of 440 to 700 Gg yr^{-1} of condensible material appears necessary to maintain the stratospheric aerosol layer (*34*). If we assume that the residence times in the stratosphere for meteoritic material and sulfuric acid are similar then the stratospheric aerosol layer would be expected to be 0.3 to 9% meteoritic material by mass. This range could be narrowed either with calibrations of PALMS data or with data from other techniques. Indeed, the upper limit of 40 Gg yr^{-1} is already difficult to reconcile with constraints posed by electron microscopy of stratospheric aerosols collected on impactors (*7*).

Our data might be used to track the origins of stratospheric aerosol particles. Besides the winter poles, aerosol particles are also produced in large numbers at the tropical tropopause (*25*). If there is meteoritic material in the particles formed during descent from high altitudes and mercury in many of the particles formed near the tropopause, then the fractions of aerosols with various compositions could provide direct tests of stratospheric transport. Meteoritic material and mercury were almost always on separate particles, but a few particles contained both. The frequency of such mixed particles might provide a test of the rate of coagulation of aerosols in the stratosphere. The observation that some particles contain neither meteoritic material

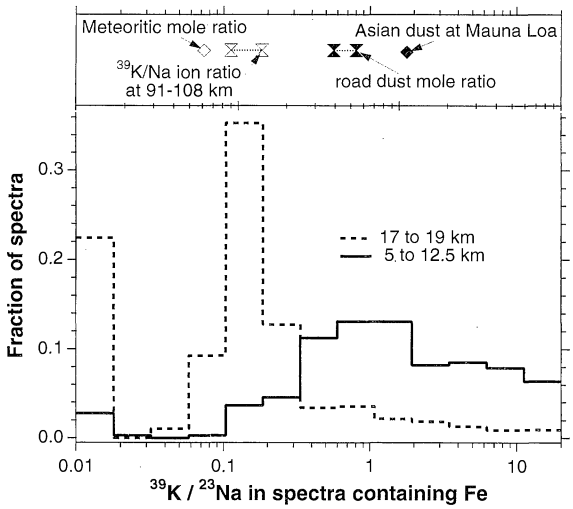

Fig. 6. The $^{39}K/^{23}Na$ ion ratio observed in aerosol particles that also contained iron for two different altitude ranges. Most of the spectra in the leftmost bin, which includes zero, did not have sufficient signal to noise to expect to see a small ^{39}K peak. Other symbols show $^{39}K/^{23}Na$ mole and ion ratios from meteoritic sources (*14, 15*) and K/Na mole ratios for surface sources (*39*). Our mass spectra are probably more sensitive to K than to Na.

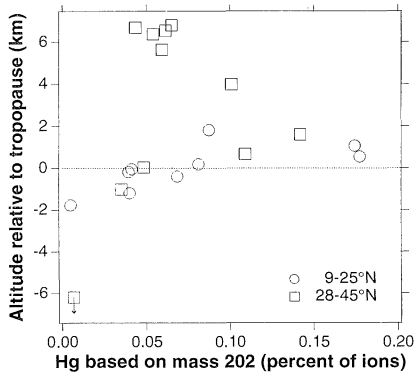

Fig. 7. The vertical profile of the percentage of mercury ions as derived from ^{202}Hg, the most abundant isotope. This peak is nearly unique for mercury in the spectra of aerosol particles. Each point is the average of the percentages in about 600 spectra. Altitudes are referenced to the tropopause altitude determined by the microwave temperature profiles. Data from 25°N to 28°N are excluded because of frequent double or ambiguous tropopauses.

nor mercury (Fig. 4B) leaves open the possibility of a third region of new particle formation in the stratosphere. The chemical composition of aerosols in the stratosphere and troposphere seem to be sufficiently distinct so that the exchange of aerosols could be tracked. For example, we observed a few particles with an unequivocal meteoritic and sulfate signal in the troposphere. Such particles most likely originated in the stratosphere. Further flight data may help assess whether stratospheric aerosols can indirectly affect the climate by serving as nuclei for cirrus clouds.

The observation of mercury at altitudes up to 19 km provides a dramatic example of how emissions from the surface can reach remote portions of the atmosphere. It also provides strong support for the estimates of a long lifetime for gaseous mercury in the atmosphere (*20*).

Finally, unusual particles could have an importance far beyond their numbers. Both cirrus clouds and polar stratospheric clouds often nucleate on only a fraction of a percent of the available aerosols. Recent research has found that ice nuclei and cirrus crystal residues at 9 to 11 km altitude have very different compositions than the majority of particles (*35*). Our data indicate that ice and cloud nuclei could come from an extremely diverse set of particles. Although unablated meteoritic material is not suitable as nuclei for nitric acid hydrates (*36*), some types of rare particles could conceivably provide freezing nuclei for polar stratospheric clouds. If nitric acid hydrates freeze only on a few nuclei, then those particles may grow larger and sediment out to denitrify the lower polar stratosphere.

Our data have thus provided a hint of how tropospheric aerosols may affect the stratosphere, but data are limited within 10° latitude of the equator, where most of the tropospheric air enters the stratosphere. Also, data from the Southern Hemispheres are needed to explore why there is more aerosol mass in the Northern Hemisphere upper troposphere (*37*) and the global influence of anthropogenic aerosols in the atmosphere.

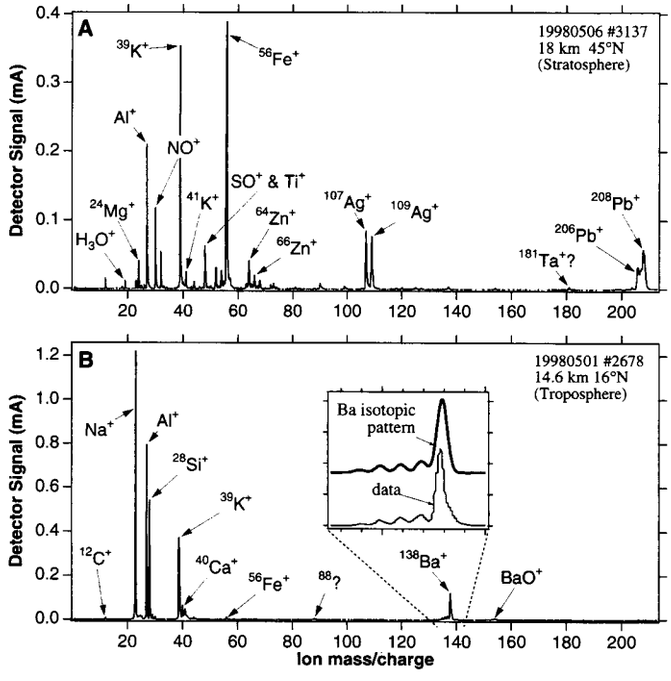

Fig. 8. Two examples of unusual particles. The inset in (**B**) shows an expanded plot of the data along with the natural isotopes of Ba convoluted with the resolution of the mass spectrometer.

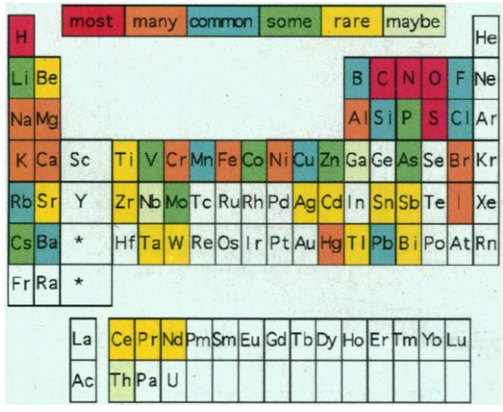

Fig. 9. Elements observed in aerosol particles at altitudes above 5 km. Frequencies are approximate because of differing ionization efficiencies. Elements with a distinctive signature of isotopes are also more likely to be unambiguously observed than those with only one isotope. Certain elements are likely to be undercounted because of spectral interferences. For example, the main isotopes of Si and Ti can be obscured by CO and SO, respectively.

References and Notes

1. J. T. Houghton *et al.*, Intergovernmental Panel on Climate Change (IPCC) Climate Change 1995: *The Science of Climate Change* (Cambridge Univ. Press, Cambridge, 1996).
2. K. S. Carslaw, T. Peter, S. L. Clegg, *Rev. Geophys.* **35**, 125 (1997).
3. D. J. Hofmann, R. S. Stone, M. E. Wood, T. Deshler, J. M. Harris, *Geophys. Res. Lett.* **25**, 2433 (1998).
4. C. E. Junge, J. E. Manson, *J. Geophys. Res.* **66**, 2163 (1961); E. K. Bigg, A. Ono, W. J. Thompson, *Tellus* **12**, 550 (1970).
5. S. C. Mossop, *Nature* **119**, 325 (1963).
6. J. P. Shedlovsky and S. Paisley, *Tellus* **18**, 499 (1966).
7. P. J. Sheridan, C. A. Brock, J. C. Wilson, *Geophys. Res. Lett.* **21**, 2587 (1994).
8. D. Hayes, K. Snetsinger, G. Ferry, V. Overbeck, N. Farlow, *ibid.* **7**, 974 (1980).
9. A. M. Middlebrook, D. S. Thomson, D. M. Murphy, *Aerosol Sci. Technol.* **27**, 293 (1997).
10. D. M. Murphy and D. S. Thomson, *ibid.* **22**, 237 (1995); ———, A. M. Middlebrook, M. E. Schein, *J. Geophys. Res.* **103**, 16485 (1998).
11. Particle numbers and volumes were derived by C. A. Brock, J. C. Wilson, J. M. Reeves, B. G. Lafleur, and D. Gesler from a condensation nucleus counter and a focused cavity aerosol spectrometer (FCAS) operated on the WB-57F. These data were corrected for refractive index and sampling bias in the FCAS. H. H. Jonsson *et al.*, *J. Atmos. Oceanic Technol.* **12**, 115 (1995).
12. R. F. Denning, S. L. Guidero, G. S. Parks, B. L. Gary, *J. Geophys. Res.* **94**, 16,757 (1989).
13. D. M. Murphy, D. S. Thomson, A. M. Middlebrook, *Geophys. Res. Lett.* **24**, 3197 (1997).
14. E. Anders and N. Gravasse, *Geochim. Cosmochim. Acta* **53**, 197 (1989).
15. U. Herrmann, P. Eberhard, M. A. Hidalgo, E. Kopp, L. G. Smith, *Space Sci.* **18**, 278 (1978).
16. D. M. Hunten, R. P. Turco, O. B. Toon, *J. Atmos. Sci.* **37**, 1342 (1980).
17. T. J. Kane and C. S. Gardner, *Science* **259**, 1297 (1993).
18. J. M. C. Plane, *Int. Rev. Phys. Chem.* **10**, 55 (1991).
19. A. Krieger and F. Arnold, *Geophys. Res. Lett.* **19**, 2310 (1992).
20. W. H. Schroeder and J. Munthe, *Atmos. Environ.* **32**, 809 (1998).
21. F. Slemr, G. Schuster, W. Seiler, *J. Atmos. Chem.* **3**, 407 (1985).
22. F. Rosebury, *Handbook of Electron Tube and Vacuum Techniques* (American Institute of Physics, New York, 1993, originally published 1964).
23. F. Slemr and H. E. Scheel, *Atmos. Environ.* **32**, 845 (1998).
24. J. S. Tokos, B. Hall, J. A. Calhoun, E. M. Prestbo, *ibid.* **32**, 829 (1998).
25. C. A. Brock, P. Hamill, J. C. Wilson, H. H. Jonsson, K. R. Chan, *Science* **270**, 1650 (1995).
26. R. L. Kaufmann, in *Physical and Chemical Characterization of Individual Airborne Particles*, K. R. Spurny, Ed. (Horwood, Chichester, 1986); P. Reilly, personal communication.
27. F. J. M. Rietmeijer and I. D. R. Mackinnon, *J. Geophys. Res.* **102**, 6621 (1997).
28. T. Novakov, D. A. Hegg, P. V. Hobbs, *ibid.*, p. 30,023.
29. J. M. Russell III *et al.*, *Geophys. Res. Lett.* **20**, 719 (1993).
30. J. C. Wilson *et al.*, *J. Geophys. Res.* **94**, 16,437 (1989); D. J. Hofmann, J. M. Rosen, J. W. Harder, J. V. Hereford, *ibid.* p. 11,252.
31. J. Zhao, O. B. Toon, R. P. Turco, *J. Geophys. Res.* **100**, 5215 (1995).
32. D. W. Fahey *et al.*, *Science* **270**, 70 (1995).
33. S. G. Love and D. E. Brownlee, *ibid.* **262**, 550 (1993); M.

Helmer, J. M. C. Plane, J. Qian, C. S. Gardner, *J. Geophys. Res.* **103**, 10,913 (1998); 4 Gg yr^{-1} is obtained from their flux after correcting the weight fraction of Fe in their calculation. An additional uncertainty in meteoritic fluxes is introduced because the actual mass available for incorporation into stratospheric aerosols may be different from the incident mass because the oxygen bound into minerals and oxides is released during ablation and then accumulated during later oxidation of iron, silicon, and other elements.

34. D. J. Hofmann, J. M. Rosen, J. M. Kiernan, J. Laby, *J. Atmos. Sci.* **33**, 1783 (1976); M. Chin and D. D. Davis, *J. Geophys. Res.* **100**, 8993 (1995); D. K. Weisenstein *et al.*, *ibid.* **102**, 13,019 (1997); M. J. Mills, thesis, University of Colorado, Boulder (1996). Condensible material converted (from 100 to 160 Gg yr^{-1} of sulfur, from oxidation of OCS and SO_2), with the assumption that 70% of the aerosol by weight is H_2SO_4.
35. Y. Chen, S. M. Kreidenweis, L. M. McInnes, D. C. Rogers, P. J. DeMott, *Geophys. Res. Lett.* **25**, 1391 (1998); J. Heintzenberg, K. Okada, J. Ström, *Atmos. Res.* **41**, 81 (1996).
36. U. M. Biermann *et al.*, *Geophys. Res. Lett.* **23**, 1693 (1996).
37. G. S. Kent, M. P. McCormick, S. K. Schaffner, *J. Geophys. Res.* **96**, 5249 (1991).
38. R. Dixon, in preparation.
39. J. J. Zieman *et al.*, *J. Geophys. Res.* **100**, 25,975 (1995); J. G. Watson *et al.*, *Aer. Sci. Technol.* **21**, 1 (1994). Range shown is from "primary geological samples."
40. The assistance of the pilots, ground crews, and staff of the WB-57F is gratefully acknowledged. This work was funded by NOAA base funding, the NASA Atmospheric Effects of Aviation Project, and the NASA Upper Atmospheric Research Program. B. Gary assisted with the MTP data analysis.

16 September 1998; accepted 2 November 1998

Structure of a Covalently Trapped Catalytic Complex of HIV-1 Reverse Transcriptase: Implications for Drug Resistance

Huifang Huang,* Rajiv Chopra,* Gregory L. Verdine,† Stephen C. Harrison†

A combinatorial disulfide cross-linking strategy was used to prepare a stalled complex of human immunodeficiency virus–type 1 (HIV-1) reverse transcriptase with a DNA template:primer and a deoxynucleoside triphosphate (dNTP), and the crystal structure of the complex was determined at a resolution of 3.2 angstroms. The presence of a dideoxynucleotide at the 3′-primer terminus allows capture of a state in which the substrates are poised for attack on the dNTP. Conformational changes that accompany formation of the catalytic complex produce distinct clusters of the residues that are altered in viruses resistant to nucleoside analog drugs. The positioning of these residues in the neighborhood of the dNTP helps to resolve some long-standing puzzles about the molecular basis of resistance. The resistance mutations are likely to influence binding or reactivity of the inhibitors, relative to normal dNTPs, and the clustering of the mutations correlates with the chemical structure of the drug.

The reverse transcriptase (RT) of HIV-1 is an important target of antiviral therapy in the treatment of acquired immunodeficiency syndrome (AIDS) (*1*). RT has two distinct enzymatic activities, an RNA- or DNA-dependent DNA polymerase and a ribonuclease (RNase) H, but current agents are directed only against the polymerase. Five of the seven inhibitors currently licensed in the United States are chain-terminating nucleoside analogs [for example, 3′-azido-2′,3′-dideoxythymidine (AZT), 2′,3′-dideoxyinosine (ddI), and 2′-deoxy-3′-thiacytidine (3TC)]. The other two inhibitors are members of a chemically diverse group of nonnucleoside RT inhibitors (NNRTIs).

HIV-1 RT is a dimer of two related chains, a 66-kD subunit (p66) and a 51-kD subunit (p51) derived from p66 by proteolytic cleavage (*2*). The two chains have in common four domains [referred to as "fingers," "palm," "thumb," and "connection" (*3*)], and p66 also has a COOH-terminal RNase H. The p66 subunit has both the polymerase and RNase H active sites. The palm contains residues critical for polymerase catalytic activity, and its folded structure resembles that of a corresponding catalytic domain in other DNA and RNA polymerases.

Emergence of resistance in patients treated with RT inhibitors is a major limitation of antiviral therapy (*4, 5*). All NNRTIs bind near the polymerase active site, in a hydrophobic pocket created by displacement of the polypeptide segment connecting palm and thumb. Viral mutations conferring resistance to these drugs can be understood readily in terms of alterations in their common binding site. In contrast, the positions of altered residues in viruses resistant to nucleoside analogs do not follow so clear a pattern (*5*). Lack of a structure for a catalytic complex of RT with template:primer and dNTP substrates has hindered understanding how site-specific changes confer resistance to particular drugs.

Previously determined RT structures include a number of NNRTI complexes and the unliganded enzyme (*3, 6–10*). The only published structure of RT with a bound template:primer is an RT•template:primer•Fab ternary complex (*6*), which shows that the primer terminus lies near three catalytically essential aspartic acid residues in the palm and that the duplex extends along the enzyme surface toward the RNase H. The position of fingers and thumb define a deep cleft, with the polymerase active site at its base. This feature, also present in crystals of RT with bound NNRTIs, has led to a model in which the 5′ extension of the template passes through the cleft, interacting with residues in the fingers and palm that are mutated in drug-resistant strains (*3, 6*). Other DNA polymerases contain a similar cleft, but recent structures of catalytic complexes show that it closes down when substrates bind and that it does not serve as a channel for polynucleotide chains (*11, 12*).

We have devised a way of isolating stalled, covalently tethered complexes of RT with template:primer, and we have crystallized one such species. In the complex described here at 3.2 Å resolution, the primer terminus is a dideoxynucleotide and thus unable to attack an incoming dNTP. The crystal of this catalytic complex contains bound dTTP in precisely the expected position for attack by the (missing) 3′ OH. The fingers domain bends, relative to other RT structures, so that various residues near the fingertips form part of the dNTP-binding site. This conformational adjustment defines the complete catalytic site and leads to a revised interpretation of the mechanism by which various mutations confer resistance to nucleoside analog drugs.

Trapping of a Catalytic HIV-1 RT–Substrate Complex

The difficulty in obtaining good crystals of an RT•template:primer•dNTP complex stems from RT's relatively modest specificity in binding to polymerizable versus nonpolymerizable sites in DNA, even in the presence of a dNTP. To overcome this problem, we chose

H. Huang and G. L. Verdine are in the Department of Chemistry and Chemical Biology, Harvard University, Cambridge, MA 02138, USA. R. Chopra and S. C. Harrison are at the Howard Hughes Medical Institute and Department of Molecular and Cellular Biology, Harvard University, Cambridge, MA 02138, USA.

*These authors contributed equally to this work.
†To whom correspondence should be addressed. E-mail: verdine@glviris.harvard.edu and schadmin@crystal.harvard.edu